

왈시-하다마다 변환과 DGT 기술을 이용한 OFDM 시스템의 PAPR 감소 및 BER성능향상을 위한 연구

공 형 윤[†] · Ho Van Khuong^{**} · 남 두 희^{***}

요 약

왈시-하다마다 변환(Walsh-Hadamard Transform, WHT)을 적용한 OFDM(Orthogonal Frequency Division Multiplexing) 변조방법은 시스템의 PAPR(Peak-to-Average Power Ratio)을 줄여주고, 시스템의 BER(Bit Error Rate) 성능을 향상시키는 장점이 있다. 그러나 기존의 이러한 왈시-하다마다 변환에 기반한 OFDM 시스템은 여전히 비교적 높은 PAPR문제가 있다. 그러므로 본 논문에서는 DGT(Data Grouping Technique)이라고 부르는 기술을 제안하고, 이 기술과 왈시-하다마다 변환 기술을 적용하여 PAPR을 더욱 줄여주는 OFDM 시스템을 설계한다. 제안한 DGT기술은 WHT-OFDM뿐만 아니라 일반 OFDM에서 PAPR을 줄여주는 방법들 중에서 큰 단점이 되는 부가정보(side information)가 성능에 대해 독립성을 가진다는 특징이 있다. 컴퓨터 시뮬레이션을 통해 제안한 시스템의 유용성을 검사하고 성능을 검증하였다.

키워드 : 주파수 분할 다중 접속, 왈시-하다마다 변환, DGT, PAPR

PAPR Reduction Improvement for WHT-based OFDM System using Data Grouping Technique

Hyung-Yun Kong[†] · Ho Van Khuong^{**} · Doo-Hee Nam^{***}

ABSTRACT

The conventional OFDM (Orthogonal Frequency Division Multiplexing) modulation can be combined with WHT (Walsh-Hadamard Transform) to reduce PAPR (Peak-to-Average Power Ratio) and improve BER (Bit Error Rate) performance. However, this WHT-based OFDM system still suffers a relatively high PAPR. Therefore, we suggest a new technique, called DGT (Data Grouping Technique) and design an OFDM system employing it and WHT to further decrease PAPR without the BER performance degradation. A salient property of DGT is the independence of the side information which is inherently a principal drawback of the well-known PAPR reduction techniques for OFDM system as well as WHT-based OFDM. The simulation programs have been also performed to verify the validity of the proposed system.

Key Word : OFDM, WH Transform, DGT, PAPR

1. Introduction

Communication channel makes signal pulses broadened in time as they travel through the channel (multi-path effect), leading to Inter-Symbol Interference (ISI). The pulse spread restricts the speed at which adjacent data pulses can be sent without overlap, thus limiting the maximum information rate of the wireless system. One technique to avoid the detrimental effect of multi-path, without sacrific-

ing the transmission rate, is OFDM (Orthogonal Frequency Division Multiplexing) modulation [1]. This is a parallel transmission scheme, where the overall frequency band is divided into a number of subbands with separate sub carriers. On each subcarrier, the modulated symbol rate is low in comparison to the channel delay spread, thus ISI can be prevented. Moreover, such subdivision makes OFDM technique attain high spectral efficiency and robustness against frequency selective multi-path fading. Therefore, it is obviously one of competitive candidates for the next generation communication systems to obtain high bit-rate without increasing the transmission bandwidth as well as decreasing the required BER performance so as to

※ 본 연구는 울산대학교 교내연구비 지원으로 이루어졌음.
[†] 정 회 원 : 울산대학교 전기전자정보시스템공학부 부교수
^{**} 준 회 원 : 울산대학교 전기전자정보시스템공학부 박사과정
^{***} 준 회 원 : 울산대학교 전기전자정보시스템공학부 석사과정
 논문접수 : 2005년 4월 6일, 심사완료 : 2005년 7월 6일

meet a drastically increasing demand of information, communication and entertainment services such as voice, data and video, etc which can be accessed anywhere at anytime. However, OFDM adversely suffers some severe problems.

First, for the frequency-selective fading channels, error bits occur as their subcarriers experience deep fades in the frequency spectrum. Although this obstacle can be solved in part by using forward error-correction (FEC) codes such as convolutional code or block code, the frequency utilization efficiency is decreased. An alternative method is to perform WHT before OFDM modulation [2]-[4]. The nature of WH transform is to send one data symbol on all subcarriers simultaneously to make the frequency diversity benefit at most. As a consequence, in addition to achieving high performance and avoiding the frequency selectivity of the channel, the WHT-based OFDM systems can decrease PAPR because the orthogonality of spreading codes guarantees the probability that all subcarriers combine constructively is very small. Moreover, [5] proposed the solution to adapting the situations where the number of subcarriers is not equal to 2^k by making use of WH matrices with different sizes. In addition, the iterative detection can be utilized to further increase BER performance at the expense of the implementation complexity [6].

Second, the conventional OFDM system (C-OFDM) has a high PAPR that tends to lessen the power efficiency of the RF amplifier. Many PAPR reducing techniques have been suggested [1] such as signal distortion techniques, typically clipping, peak windowing and peak cancellation; coding techniques, SLM (Selected Mapping Method) and PTS (Partial Transmit Sequence). Moreover, the above mentioned WHT as well as the selection of the sets of spreading sequences between Walsh-Hadamard and complementary sequences [4] is an effective way to deal with PAPR problem. However, similar to SLM and PTS, the technique in [4] suffers the severe bit error performance degradation due to the erroneous side information (SI) which contains the information of selected spreading codes at the transmitter. In general, applying these PAPR reduction techniques is a cost of increasing transmission bandwidth, deteriorating system's performance and making system more complicated.

As we see, WHT-based OFDM system is better than C-OFDM system in many aspects such as high performance and low PAPR. However, PAPR of WHT-based OFDM system is still high. Therefore, we propose DGT whose function is to choose a proper set of phase control gains for groups to attain a lowest PAPR before trans-

mitting the signal over the channel. Moreover, the receiver doesn't require SI of phase set which was embedded into transmitted data to decode the original data and thus, the system performance is independent of SI. This is the proposed technique's prominent advantage over SLM, PTS [1] and the sequence selection [4] whose SI has an adverse effect on system performance if it is not correctly recovered.

The rest of this paper is organized as follows. Section 2 discusses details of the proposed system. The simulation results are presented in section 3 and part 4 is conclusion of the paper.

2. Proposed System Structure (P-OFDM)

2.1 Transmitter model

The suggested system block diagram is shown in (Fig. 1). First of all, the i^{th} data block of modulated symbols with symbol duration T_S is serial-to-parallel converted into I branches which is subdivided into M groups of length $L-1$, except the first group of length L , namely B_m where $m=1, \dots, M$ as in (Fig. 2).

The relation of M , I and L is given by

$$I = M(L-1) + 1 \tag{1}$$

Then the groups with indices from 2 to M are added one more symbol b_m ($m=1, \dots, M-1$) taken from the optimizer to produce a lowest PAPR among its all possible combinations of vector $b=[b_1 \ b_2 \ \dots \ b_{M-1}]$.

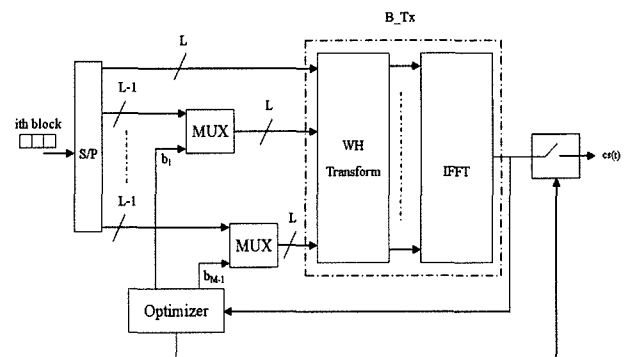


(Fig. 1) Proposed transmitter model

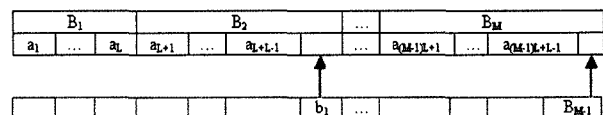


(Fig. 2) Structure of M groups
 a_u : data symbols, b_m : phase control factors

The symbols b_m have no meaning at the receiver because the purpose of inserting b_m into useful data is only to control the phase of transmitted signal. Therefore, PAPR reduction is paid only for the decrease in spectral efficiency. Compared to the system without using the PAPR reducing technique, that is, all groups consisting of L data symbols, the bandwidth loss of this system can be calculated as follows

$$\text{bandwidth loss} = 1 - \frac{M(L-1)+1}{ML} = \frac{M-1}{ML} \quad (2)$$

Here ML is chosen to be equal to the number of sub-carriers N . If ML is large, then the above loss is negligible.

We denote the input vector and output vector of WH transform block by a and w , respectively

$$a = [a_1 \ a_2 \ \dots \ a_N]^T \quad (3)$$

$$w = d \ a \quad (4)$$

where d is Walsh-Hadamard matrix, each column of which is considered as the spreading code of the symbol a_k in frequency domain.

$$d = \begin{bmatrix} d_{1,1} & \dots & d_{1,N} \\ \vdots & & \vdots \\ d_{N,1} & \dots & d_{N,N} \end{bmatrix} \quad (5)$$

The nature of B_Tx (see Fig. 1) is illustrated in (Fig. 3), where each symbol a_k ($k=1, \dots, N$) is replicated N times and multiplied with $d_{n,k}$ ($n=1, \dots, N$). The resulting signal is given below:

$$u_{n,k} = a_k d_{n,k} \quad ; n=1, \dots, N; k=1, \dots, N \quad (6)$$

where $d_{n,k}$ is the n^{th} chip of the k^{th} spreading code and a_k denotes the k^{th} symbol. Then these $u_{n,k}$ are multi-carrier modulated by N subcarriers with frequencies chosen to be an integer multiple of block rate. In this system, we adopt

$$\Delta f = \frac{1}{NT_s} \quad (7)$$

Here, Δf describes the frequency distance between two adjacent sub-carriers and the selecting Δf as above assures that all subcarriers are orthogonal. This is a mandatory

condition for an OFDM system.

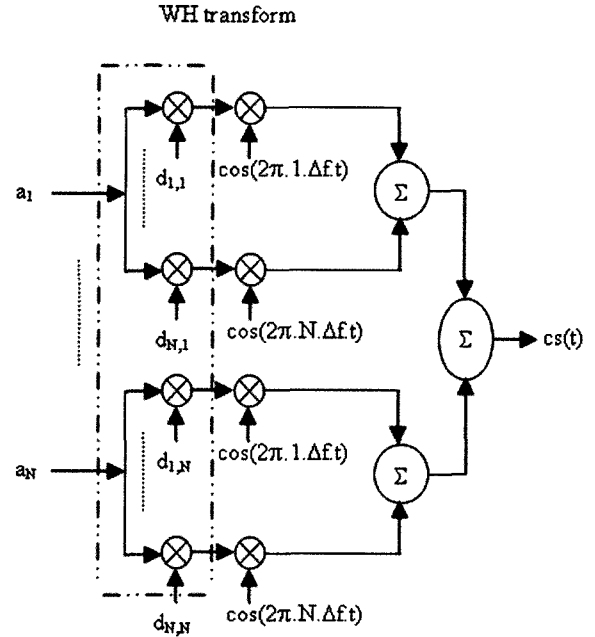


(Fig. 3) Detail block diagram of B_Tx

Subsequently, the signals from all parallel branches after spread in frequency domain by d_k are summed together which results in a composite signal as follows

$$cs(t) = \sum_{i=-\infty}^{\infty} \sum_{k=1}^N \sum_{n=1}^N A a_k(i) d_{n,k} \cos(2\pi n \Delta f t) p(t - iNT_s) \quad (8)$$

where $p(t)$ is a unit-amplitude rectangular pulse over the interval $[0, NT_s]$; A : the amplitude of each sinusoid signal; i : the i^{th} block.

In practice, multi-carrier modulation block can be implemented efficiently by IFFT (Inverse Fast Fourier Transform). Therefore, the whole block diagram of (Fig. 3) can be replaced by a WH transform followed by IFFT as in (Fig. 1).

As usual, N -point IFFT is used to perform multi-carrier modulation which is equivalent to the sampling the continuous signal $cs(t)$ with the sampling period $1/N\Delta f$. However, this sampling period is not short enough to capture the peaks of the signal $cs(t)$ and thus leading to the large error in computing PAPR compared to the true PAPR value. Therefore, to increase the degree of accuracy of calculated PAPR, we follow [7] that ensures the computed PAPR to be almost approximate with the continuous PAPR value by applying oversampling with a factor of greater than four. In this paper, the signal is oversampled by a factor of 8. Therefore, the sampling duration is given by

$$T_{\text{sampling}} = \frac{T_s}{8} \tag{9}$$

To implement this intention by IFFT, we pad $7N$ zero samples at the tail of vector w and take $8N$ -point IFFT on the resulting vector to have the signal $cs(nT_{\text{sampling}})$ in the discrete form which is used to calculate the PAPR defined as

$$PAPR = \frac{\max_{0 \leq m < 8N} |cs(mT_{\text{sampling}})|^2}{\text{mean}_{0 \leq m < 8N} |cs(mT_{\text{sampling}})|^2} = \frac{\max_{0 \leq m < 8N} |cs(mT_{\text{sampling}})|^2}{\sum_{m=0}^{8N-1} |cs(mT_{\text{sampling}})|^2} \cdot 8N \tag{10}$$

where $cs(mT_{\text{sampling}})$ is the transmitted signal during one OFDM symbol. For the C-OFDM, PAPR can reach the maximum value of N in the worst case as all subcarriers combine coherently.

It is easy to illustrate that there exists the data symbol combinations as an input of WH transform section which produce a low PAPR. <Table 1> giving an example of tested all possible combinations for case of $N=4$ shows that there are only 4 combinations of the vector a with the generated large PAPR. These combinations are easily avoided by the optimizer. Therefore, the operation mechanism of the optimizer is to compute PAPR for all possible combinations of vector b and store in its buffer. When the PAPR computation is finished, the optimizer selects an optimal combination of b corresponding to the lowest PAPR and turns the switch on to send $cs(t)$ to the next block.

<Table 1> PAPR for different data symbol combinations for $N=4$

Input data combinations	Average PAPR
[0 1 1 1], [1 0 1 1], [0 1 0 0], [1 0 0 0]	1.3762
Others	≈0.9444

One of OFDM system's outstanding advantages is capability of suppressing completely ISI (Inter-Symbol Interference) caused by multi-path dispersion channel. This is validated by inserting a guard interval Δ with length greater than the maximum delay spread of the channel. Although this interval reduces the spectral efficiency, the complexity of receiver is significantly decreased. Finally, the integrated signal $cs(t)$ is transmitted after RF-up conversion.

2.1.2. Channel Model

The complex equivalent low-pass time-variant impulse

response of p -path frequency selective Rayleigh fading channel is given by [8]

$$h(t, \tau) = \sum_{i=1}^p g_i(t) \delta(t - \tau_i)$$

where $g_i(t)$, τ_i are gain and delay of the i^{th} path in the power delay profile of channel. This paper assumes the channel to be WSSUS (Wide Sense Stationary Uncorrelated Scattering), and thus, $g_i(t)$ is a mutually independent complex Gaussian random process with zero mean, variance $\sigma_{g_i}^2$ (Jakes-like algorithm for $g_i(t)$ coefficients generation found in [8]) and the autocorrelation function [8]:

$$R_{g_i}(\Delta t) = \sigma_{g_i}^2 \cdot J_0(2\pi f_{d\max} \Delta t)$$

in which $J_0(\cdot)$ and $f_{d\max}$ are the zero-order Bessel function of the first kind and maximum Doppler frequency, respectively.

If the condition $\Delta f \ll B_c \ll BW$ (B_c : coherent bandwidth of channel, BW : total bandwidth of system) is satisfied, then each subcarrier only undergoes a flat fading. Therefore, the frequency-selective Rayleigh fading channel's transfer function H_n can be modeled as

$$H_n = \alpha_n e^{j\phi_n} \tag{11}$$

where α_n is the amplitude and ϕ_n the phase in the n^{th} sub-channel or the n^{th} subcarrier due to fade; α_n are statistically independent Rayleigh random variables and ϕ_n are uniform random variables over the interval $[0, 2\pi]$. In this paper, α_n and ϕ_n are assumed to be unchanged during each symbol interval but fluctuate over longer periods of time.

2.1.3 Receiver model

The received signal after frequency down-converted, guard-interval removed and analog-to-digital transformed is processed sequentially as shown in (Fig. 4). First, the discrete signal $r(m)$ given by

$$r(m) = \sum_{k=1}^N \sum_{n=1}^N A \alpha_n e^{j\phi_n} e^{j2\pi m \Delta f T} a_k d_{n,k} + v(m) \tag{12}$$

is N -point fast Fourier transformed for multi-carrier demodulation, where α_n and ϕ_n are in (11); $v(m)$ is a AWGN component with zero mean and variance σ_v^2 ; T : sampling period.

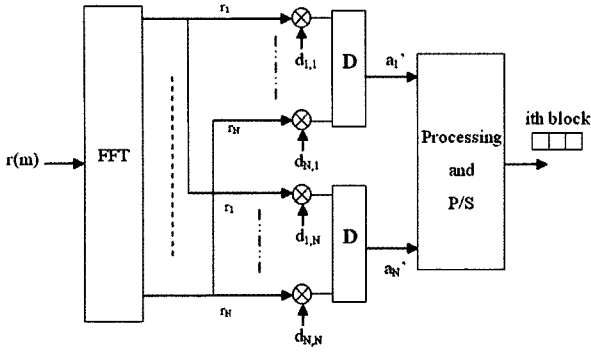


(Fig. 4) Block diagram of the proposed receiver; D: detector

The resultant signal r is of the following form with an assumption that the frequency synchronization is perfect:

$$\begin{bmatrix} r_1 \\ \vdots \\ r_N \end{bmatrix} = A \begin{bmatrix} a_1 \\ \vdots \\ a_N \end{bmatrix} \otimes \begin{bmatrix} H_1 \\ \vdots \\ H_N \end{bmatrix} + \begin{bmatrix} V_1 \\ \vdots \\ V_N \end{bmatrix} \quad (13)$$

where

$$r_n = \sum_{k=1}^N A \alpha_n e^{j\theta_n} a_k d_{n,k} + V_n, \quad n=1, \dots, N \quad (14)$$

and noise vector $V=[V_1 \ V_2 \ \dots \ V_N]^T$ is FFT of $v=[v(1) \ v(2) \ \dots \ v(N)]^T$; $(\cdot)^T$: transpose operator; d : Walsh-Hadamard matrix; a : vector of the original data symbols; \otimes : element-by-element product; H : matrix of channel coefficients with each element given by (11).

Eq. (13) shows that there is interference among data symbols, called IDSI (InterData-Symbol Interference), which degrades the performance of the system.

Before the a_k is decoded, r is despread by its own codes $d_k = [d_{1,k}, d_{2,k}, \dots, d_{N,k}]^T$ to produce a vector:

$$y_k = [y_{1,k}, y_{2,k}, \dots, y_{N,k}]^T = r \otimes d_k \quad (15)$$

Then we apply the MMSE (Minimum Mean Square Error) condition [9] on y_k to recover a_k as follows

$$a'_k = \sum_{n=1}^N e_n y_{n,k} \quad (16)$$

where e_n are combination coefficients given by [10]:

$$e_n = \frac{H_n^*}{|H_n|^2 + 1/SNR} \quad (17)$$

in which SNR is signal-to-noise power ratio.

It is straightforward to infer from (17) that MMSE detector minimizes the IDSI and Gaussian noise while best exploiting the frequency diversity benefits.

Finally, the detected symbols a'_k are passed through a processing block and parallel-to-serial transformed to recover the original data block. The function of the processing block is to simply remove the last bits of the recovered data blocks with indices greater than 2. To explain its mechanism more clearly, we take a simple example of the system with $N=8$, two BPSK-modulated data groups and b_m is chosen from the set $\{+1, -1\}$ as follows.

Group index	1				2			
Original data	1	-1	1	1	1	1	-1	

The vector a as the input to the WHT block (see Fig. 1) is created by keeping the first group unchanged but inserting a bit b_l into the last position of the second group as the side information. The resulting stream is given by

Group index	1				2			
Transmitted data a	1	-1	1	1	1	1	-1	-1



Now we have two possible values of b_l as -1 or $+1$. For each value, the optimizer will calculate the PAPR and finally, it selects b_l which creates the lowest PAPR to fill in the last location in the second group. In this example, we assume b_l to be -1 .

Assuming that the received vector $a' = [a'_1 \ a'_2 \ \dots \ a'_N]$ is $[+1 \ -1 \ +1 \ +1 \ +1 \ +1 \ -1 \ +1]$. Then the processing block performs the reversed steps of the above. First, it remains the first group and afterward removes b_l out of the received block.

Group index	1				2			
Output of processing block	1	-1	1	1	1	1	-1	

As a consequence, even though the SI bit is wrongly decoded, the system performance is not affected; that is, it is independent of SI (vector b). This is a prominent feature of DGT over other PAPR-reducing techniques such as PTS and SLM in [1] and sequence selection in [4] which strongly depend on SI .

3. Simulation results and discussions

In this part, we will present simulation results of three systems: P-OFDM, C-OFDM and WHT-based OFDM (WH/OFDM) in a frequency selective fading channel. The complex baseband-equivalent model is used for simulation. Assuming that the guard interval is longer than the maximum delay spread of the channel to completely suppress ISI and each sub-carrier only experiences a flat Rayleigh fading given in Eq. (11) with equal power expectation values.

To be convenient for the goal of comparison among the systems, computer simulations only examine the MMSE detectors. Moreover, BPSK transmission and no channel coding are considered and each element of the phase control vector b is selected from the set $\{-1, +1\}$. In addition, the number of subcarriers is limited to $N=16$ and 32 for low computation complexity. Furthermore, the channel state information is assumed to be perfectly estimated at the receiver.

<Table 2> PAPR's parameters comparison for C-OFDM, WH/OFDM and P-OFDM ($N=32-2$ means 32 subcarriers and 2 groups)

P-OFDM	Mean	Variance	Max	Min
N=16-2	2.2959	0.1437	4.5011	1
N=16-4	1.9961	0.0656	3.7169	1
N=16-8	1.6732	0.0521	2.2659	1
N=32-2	2.9647	0.2894	7.0368	1.6173
N=32-4	2.6237	0.1628	6.7106	1.5569
N=32-8	2.2725	0.1183	6.1221	1
C-OFDM	Mean	Variance	Max	Min
N=16	3.7102	1.3295	16.0000	1.7071
N=32	4.3643	1.4969	18.0000	1.9321
WH/OFDM	Mean	Variance	Max	Min
N=16	2.5820	0.3142	6.1594	1
N=32	3.2316	0.4708	8.2103	1.6928

The statistical data of PAPR for the different number of subcarriers $N=16, 32$ is illustrated in <Table 2> in which PAPR is calculated for 500000 data symbol combinations whose components are randomly selected with a uniform possibility and the sample number per an OFDM symbol is $8N$. Moreover, the group number under investigation is $M=2, 4$ and 8 . *It is noted* that our system becomes the conventional WHT-based OFDM if $M=1$. As we can see, for any value of N and M , the PAPR of the proposed

system is considerably better than that of C-OFDM and WH/OFDM, particularly, its PAPRs fluctuate slightly around the mean value (small variance), for example: P-OFDM's average PAPR is 2.9647 ($N=32-2$) while 4.3643 for C-OFDM and P-OFDM's PAPR variance is 0.2894 in contrary to 1.4969 for C-OFDM. Furthermore, other parameters such as maximum PAPR and minimum PAPR are considerably less than those of C-OFDM and WH/OFDM.

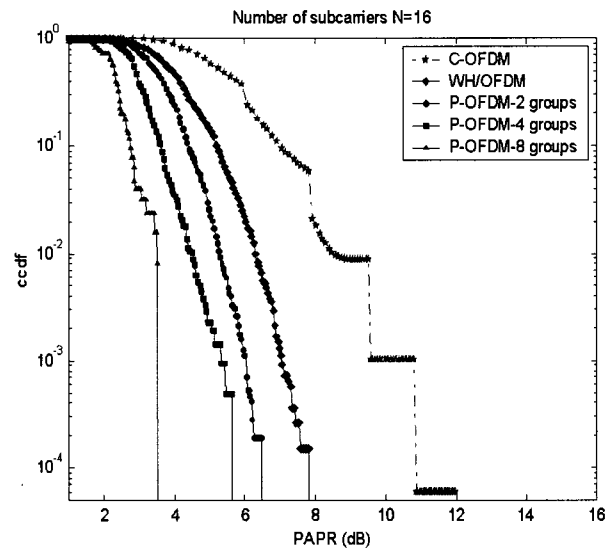


(Fig. 5) ccdf of PAPR for C-OFDM, WH/OFDM and P-OFDM (ccdf = $\Pr[\text{PAPR} > \text{PAPR}_0]$)

<Table 2> also shows that PAPR's parameters increase with respect to an increase of N . With small variance, the new system demonstrates that its PAPR is less sensitive with input data combinations than C-OFDM or WH/OFDM and changes almost slowly. In addition, the more groups the input data is divided into, the more effective the PAPR reduction. For P-OFDM, the probability that PAPR is greater than 6.1221 is zero for the case of 32 subcarriers and 8 groups; and similarly 2.2659 for $N=16$ and $M=8$. However, the cost to be paid for this improvement in PAPR is the bandwidth waste but BER performance is not degraded because it is not dependent of SI (see Figs. 7-8).

In order to have an insightful and intuitive view on PAPR statistics, Figs. 5-6 plot ccdf (complementary cumulative density function) of PAPR for $N=16, 32$ for $M=2, 4, 8$ groups. Once again these figures reveal a dramatic improvement in alleviating a high PAPR in the new system over C-OFDM and WH/OFDM. For instance, a PAPR reducing enhancement of the P-OFDM is about 5dB over C-OFDM and approximately 1.5dB over WH/OFDM at ccdf of 10^{-4} for $N=16$ and $M=2$.

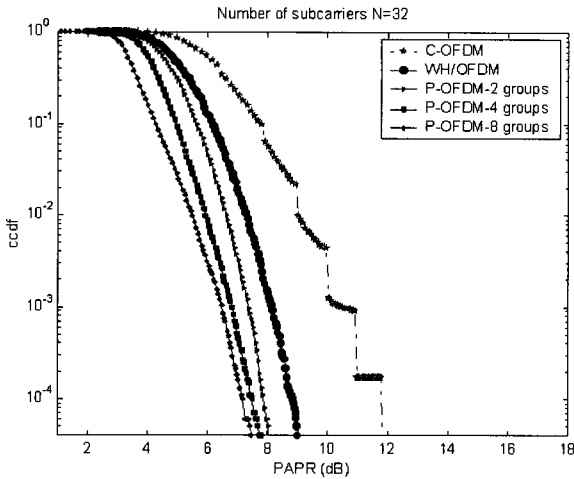


(Fig. 6) cdf of PAPR for C-OFDM, WH/OFDM and P-OFDM

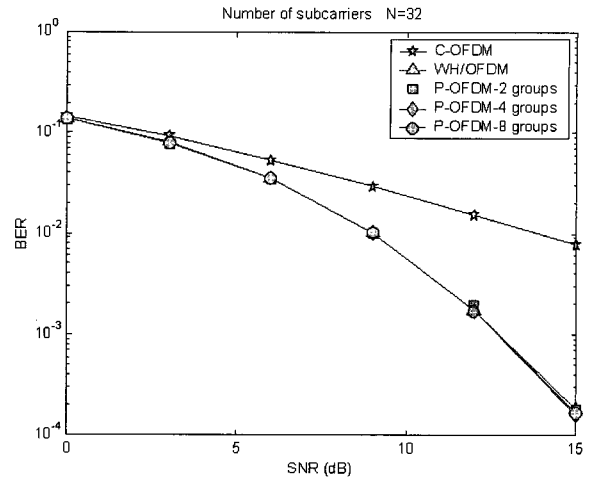


(Fig. 8) BER Performance of C-OFDM, WH/OFDM and P-OFDM for N=32

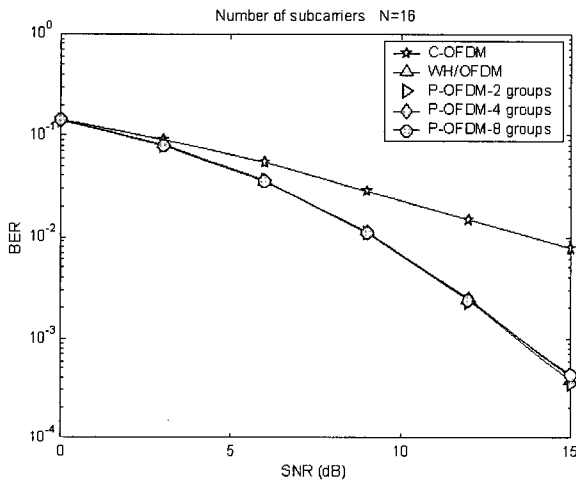


(Fig. 7) BER Performance of C-OFDM, WH/OFDM and P-OFDM for N=16

BER performance in frequency selective Rayleigh fading channel with AWGN illustrated in Figs 7-8 shows that the performance of C-OFDM is significantly degraded by fading channel. However, for P-OFDM, due to frequency diversity benefit, its performance is considerably improved in comparison to C-OFDM with approximately 5dB SNR gain at BER 10^{-2} for any N and M . Furthermore, BER enhancement accelerates with respect to an increase in the subcarrier number while C-OFDM's BER is almost unchanged. This is because the frequency diversity gain also increases according to N . Obviously, this property can not be found in C-OFDM. Figs. 7-8 also demonstrate that there is no performance degradation for P-OFDM as the number of groups increases because as reasoned in part 2.1 that P-OFDM's performance is independent on the number of groups. Therefore, the performance of P-OFDM is also identical to that of WH/OFDM.

4. Conclusion

WHT-based OFDM system outperforms the conventional OFDM system in both aspects of BER performance and PAPR reduction without bandwidth expansion. By subdividing the input symbol stream into smaller groups, our proposed system corrects the disadvantage of WHT-based OFDM in high PAPR. The larger the number of groups, the more PAPR reduction increases and the less bandwidth utilization efficiency but not deteriorate error bit probability performance. Therefore, our system is suitable to apply for the transmitters of high frequency amplifiers with small dynamic range and operated in harsh environments as multi-path fading channels.

References

- [1] Richard van Nee, Ramjee Prasad, "OFDM for Wireless Multimedia Communications", Artech House, 2000.
- [2] B.M. Popovic, "Spreading sequences for multicarrier CDMA systems", IEEE Trans. Commun., Vol.47, Issue 6, pp.918-926, June, 1999.
- [3] Yan Wu, Chin Keong Ho, Sumei Sun, On some properties of Walsh-Hadamard transformed OFDM", VTC 2002-Fall, Vol.4, 24-28 Sept., 2002. pp.2096-2100.
- [4] H. Ochiai, H. Imai, "OFDM-CDMA with peak power reduction based on the spreading sequences", ICC 98, Vol.3, pp.1299-1303, 7-11 June, 1998.
- [5] Z. Dlugaszewski, K. Wesolowski, "WHT/OFDM - an improved OFDM transmission method for selective fading channels", SCVT-2000, pp.144-149, 19 Oct., 2000.

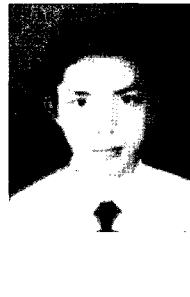
- [6] Zhongding Lei, Yan Wu, Chin Keong Ho, Sumei Sun, Ping He, Yuan Li, "Iterative detection for Walsh-Hadamard transformed OFDM", VTC 2003-Spring, Vol.1, pp.637-640, 22-25 April, 2003.
- [7] C. Tellambura, "Computation of the Continuous-Time PAR of an OFDM Signal with BPSK Subcarriers", IEEE Communications Letters, Vol.5, pp.185-187, May, 2001.
- [8] James K. Cavers, "Mobile Channel Characteristics", Kluwer Academic Publishers, 2000.
- [9] D.N. Kalofonos, M. Stajanovic, J.G. Proakis, "On the performance of Adaptive MMSE Detectors for a MC-CDMA System in Fast Fading Rayleigh Channels", The ninth IEEE International Symposium on Personal, Indoor and Mobile Radio Communications, Vol.3, pp.1309-1313, 8-11 Sept., 1998.
- [10] John G. Proakis, "Digital communications", Fourth Edition, McGraw-Hill, 2001.



공형운

e-mail : hkong@mail.ulsan.ac.kr
 1989년 미국 New York Institute of Technology 전자공학과(학사)
 1991년 미국 Polytechnic University 전자공학과(석사)
 1996년 미국 Polytechnic University 전자공학과(박사)

1996년~1996년 LG전자 PCS 팀장
 1996년~1998년 LG전자 회장실 전략사업단
 1998년~현재 울산대학교 전기전자정보시스템공학부 부교수
 관심분야: 코딩(LDPC, Turbo) 및 모듈레이션(OFDM, QAM), 멀티코드, Wireless Sensor Network 등



Ho Van Khuong

e-mail : khuongho21@yahoo.com
 2001년 베트남 HoChiMinh City University of Technology 전기전자공학과(학사)
 2003년 베트남 HoChiMinh City University of Technology 전기전자공학과(석사)
 2004년~현재 울산대학교 전기전자정보시스템공학과 박사과정

관심분야: OFDM, MC-DMA, 협력 통신, 채널 추정



남두희

e-mail : duheeya@mail.ulsan.ac.kr
 2004년 울산대학교 전기전자정보시스템공학부(학사)
 2004년~현재 울산대학교 전기전자정보시스템공학과 석사과정

관심분야: LDPC, MC-CDMA, 멀티코드, 협력 통신, 센서 네트워크